Acta Oceanol. Sin., 2019, Vol. 38, No. 9, P. 35–47
https://doi.org/10.1007/s13131-019-1383-9
http://www.hyxb.org.cn
E-mail: hyxbe@263.net

Numerical simulations and comparative analysis for two types of storm surges in the Bohai Sea using a coupled atmosphere-ocean model

Yong Li[1, 2], Xin Chen[3], Xingyu Jiang[1, 2], Jianfen Li[1, 2], Lizhu Tian[1, 2*]

[1] Tianjin Centre, China Geological Survey, Tianjin 300170, China

[2] Key Laboratory of Coast Geo-environment, China Geological Survey, Tianjin 300170, China

[3] Beijing Engineering Research Center of Safety and Energy Saving Technology for Water Supply Network System, China Agricultural University, Beijing 100083, China

Received 18 April 2018; accepted 8 October 2018

Abstract

The Bohai Sea is extremely susceptible to storm surges induced by extratropical storms and tropical cyclones in nearly every season. In order to relieve the impacts of storm surge disasters on structures and human lives in coastal regions, it is very important to understand the occurring of the severe storm surges. The previous research is mostly restricted to a single type of storm surge caused by extratropical storm or tropical cyclone. In present paper, a coupled atmosphere-ocean model is developed to study the storm surges induced by two types of extreme weather conditions. Two special cases happened in the Bohai Sea are simulated successively. The wind intensity and minimum sea-level pressure derived from the Weather Research and Forecasting (WRF) model agree well with the observed data. The computed time series of water level obtained from the Regional Ocean Modeling System (ROMS) also are in good agreement with the tide gauge observations. The structures of the wind fields and average currents for two types of storm surges are analyzed and compared. The results of coupled model are compared with those from the uncoupled model. The case studies indicate that the wind field and structure of the ocean surface current have great differences between extratropical storm surge and typhoon storm surge. The magnitude of storm surge in the Bohai Sea is shown mainly determined by the ocean surface driving force, but greatly affected by the coastal geometry and bathymetry.

Key words: the Bohai Sea, extratropical storm surge, typhoon storm surge, coupled atmosphere-ocean model, WRF, ROMS

Citation: Li Yong, Chen Xin, Jiang Xingyu, Li Jianfen, Tian Lizhu. 2019. Numerical simulations and comparative analysis for two types of storm surges in the Bohai Sea using a coupled atmosphere-ocean model. Acta Oceanologica Sinica, 38(9): 35–47, doi: 10.1007/s13131-019-1383-9

1 Introduction

Storm surge is defined as the abnormal change in sea level, which associated with either extratropical or tropical storm. The storm surge may cause significant human life losses and severe damages to coastal structures. The Bohai Sea is susceptible to storm surges induced by extratropical storms and cyclones. The extratropical storm surges are mainly caused in spring, autumn and winter and the typhoon storm surges are mainly caused in summer (Wu et al., 2002; Fu et al., 2013; Mo et al., 2016; Ding and Wei, 2017; Li et al., 2017).

Many researchers show great interest to understand severe storm surges in the Bohai Sea. By comparison, the extratropical storm surge has much greater effect on the Bohai Sea than typhoon storm surge and numerical simulation of extratropical storm surge is one of the emphases for research (Wu et al., 2002). Based on the zeroth-order model of the ultra-shallow water storm surge theory, a numerical investigation of the Bohai Sea wind surges was first made by Sun et al. (1979, 1982). Entering the first decade of twenty-first century, the related numerical research is endless and the results are also numerous. Li et al. (2010) developed a numerical model of storm surge affected by the coupling of wind and wave. The Fifth-Generation Mesoscale Model (MM5) was used to calculate wind field and the Putian Station Method was adopted to get wave factors. Furthermore, the SWAN (simulating waves nearshore) wave model was added to the numerical model and the wave-induce radiation stress on storm surge was studied (Li et al., 2015). Zhao and Jiang (2011) took the different major tracks, pressure field and high wind period into consideration and constructed several scenarios to describe the actual situation of cold-air outbreaks. Based on the results modeled by the Finite-Volume Coastal Ocean Model (FVCOM), the influence of various cold-air outbreaks on the maximum surge in the Bohai Sea and the probability of the surge elevation at typical tide gauges were investigated. Using the Advanced Circulation (ADCIRC) model and atmospheric reanalysis data, the extratropical storm surge occurred in December 2010 was simulated by Fu et al. (2011). With similar method, numerical study on deepwater channel influenced by negative storm surge and its features in the Bohai Sea was carried out (Fu et al., 2014). Using FVCOM, a hindcast of typical extratropical storm surge oc-

Foundation item: The National Natural Science Foundation of China under contract Nos 41372173 and 51609244; the Geological Survey Projects of China Geological Survey under contract No. 121201006000182401.
*Corresponding author, E-mail: tjtlzct@163.com

curring in the Bohai Sea in October 2003 was performed by Ding and Ding (2014). The storm surge model was forced by winds obtained from the Weather Research and Forecasting (WRF) model simulation. Thereafter, the model was used to study the impact of land reclamation on storm surges in the Bohai Sea (Ding and Wei, 2017). The Regional Ocean Modeling System (ROMS) was adopted to study storm surges induced by cold waves in Mo et al. (2016). The role of wind direction, wind speed, wind duration, extratropical storm and tide-surge interaction was investigated by conducting different sensitivity experiments. Also, using ROMS, Li et al. (2016) developed a storm surge and inundation numerical model for the west zone of Bohai Bay, in which the QSCAT/NCEP (Quick Scatter Meter/National Center for Environmental Prediction) blended wind data was used to calculate the wind stress. Thereafter, Li et al. (2017) developed a coupled atmosphere-ocean model which was successful in simulating the extratropical storm surge happened in the Bohai Bay. As a whole, numerical study about the typhoon storm surge for the Bohai Sea is rare and applications of coupled atmosphere-ocean model for extratropical storm surge are still at the initial stage.

Generally, the foreign scholars have done much research on the coupled atmosphere-ocean model and have obtained many achievements, while the domestic research in this area is slightly behind. Warner et al. (2008, 2010) developed a Coupled Ocean-Atmosphere-Wave-Sediment Transport (COAWST) modeling system. The system includes the ROMS ocean model, the WRF atmosphere model, the SWAN wave model and the Community Sediment Transport Model (CSTM). The COAWST system was used to identify model sensitivity by exchanging prognostic variable fields between different model components during an application to simulate Hurricane Isabel in 2003. After that, sensitivity experiments were performed to assess the impacts of coupling on the predictions of the atmosphere, ocean and wave environments during the occurrence of the Hurricane Ivan in 2004 (Zambon et al., 2014). Moreover, Hurricane Ida in November 2009 and Typhoon Muifa in August 2011 were also simulated by using the COAWST system (Olabarrieta et al., 2012; Liu et al., 2015). Based on the GRAPES (Global and Regional Assimilation and Prediction System) regional typhoon model (GRAPES_TYM) and ECOM-si (estuary, coast and ocean model (semi-implicit)), Sun et al. (2014) developed a mesoscale coupled atmosphere-ocean model to simulate the Typhoon Muifa. Based on MM5, POM (Princeton Ocean Model) and WW3 (Wave Watch III), a regional atmosphere-ocean-wave coupled system was set up and the coupled system was tested in a study of typhoon processes in the South China Sea (Guan et al., 2012). Using WRF, FVCOM and SWAN, a coupled atmosphere-ocean-wave model was developed and applied in the simulation of the Typhoon Rammasun by Wang et al. (2016). So far, the coupled atmosphere-ocean model has been mainly used to simulate the storm surges caused by tropical cyclone (TC).

As mentioned above, the Bohai Sea is susceptible to extratropical storm surge and typhoon storm surge. Many scholars have done their research from different angles (e.g., Sun et al., 1979; Li et al., 2010, 2017; Fu et al., 2014; Ding and Ding, 2014; Mo et al., 2016). But until now, few studies have investigated the differences and similarities between extratropical storm surge and typhoon storm surge. Meanwhile, the research contents mainly focus on storm surge elevation, with less attention to wind and flow fields. In this paper, a coupled atmosphere-ocean model is developed to investigate the differences and similarities between the two types of storm surge in the Bohai Sea. The simulation results, such as wind intensity and direction, average wind stress, average surface currents and so on, are analyzed and compared between the two types of storm surges. The following section briefly introduces the WRF atmosphere model, ROMS ocean model and the coupling methods. Section 3 explores the model domains and configuration settings. In Section 4.1, the extratropical storm surge occurred in October 2003 is simulated and analyzed. In Section 4.2, the typhoon storm surge occurred in August 1992 is simulated and the results of typhoon storm surge are compared with those of the extratropical storm surge. Finally, summary and conclusions are given in Section 5.

2 Numerical models

2.1 *WRF*

The WRF is a next-generation mesoscale numerical weather prediction model. The WRF is presented by the National Centre for Atmospheric Research (NCAR), who collaborates with many other research institutes. The model is a non-hydrostatic, quasi-compressible atmospheric model and has been widely utilized for both realistic and idealized weather forecasts. A variety of options for microphysics, cumulus, boundary layers and radiation physical processes are available in WRF (Skamarock et al., 2008; Liu et al., 2017). Much research indicates that it is suitable for weather simulations across scales ranging from meters to thousands of kilometres. Here, the Version 3.7.1 WRF model is adopted to couple with the ROMS ocean model.

2.2 *ROMS*

The ROMS model is a free surface, terrain-following, primitive equations ocean model. Based on finite difference method, ROMS solves the Reynolds-Averaged Navier-Stokes (RANS) equations with hydrostatic and Boussinesq assumptions. The model uses a horizontal curvilinear grid system and stretched terrain-following coordinate in a vertical array. It has been widely used for the prediction of ocean hydrodynamic environment (Haidvogel et al., 2008; Lim et al., 2013). The ROMS model of Version 3.6 is coupled with the WRF model in this study.

2.3 *Coupled atmosphere-ocean numerical model*

WRF and ROMS are coupled using the Model Coupling Toolkit (MCT) and the Spherical Coordinate Remapping Interpolation Package (SCRIP). As shown in Fig. 1a, the MCT is used to handle the passing of variables between the coupled models, as well as regridding and time averaging. Data are exchanged between WRF and ROMS by MCT at initialization process. After that, the data exchange occurs between the models at a defined synchronization point. In addition, mesh points in each two models has to be interpolated for data exchange by the MCT. The SCRIP is utilized to compute the interpolation weights for remapping and interpolating fields between different grid systems. The weights are calculated by a bilinear interpolation method and are read in for use during the coupled iteration process.

At the defined synchronization point, the sea surface stresses and net heat fluxes are passed from WRF to ROMS. Meanwhile, the sea surface temperature is passed from ROMS to WRF. The variables that are exchanged in coupled model are shown in Fig. 1b.

The surface roughness is computed in WRF based on the relation of roughness length to wind stress (Charnock, 1955):

$$z_0 = z_c \frac{u_*^2}{g}, \tag{1}$$

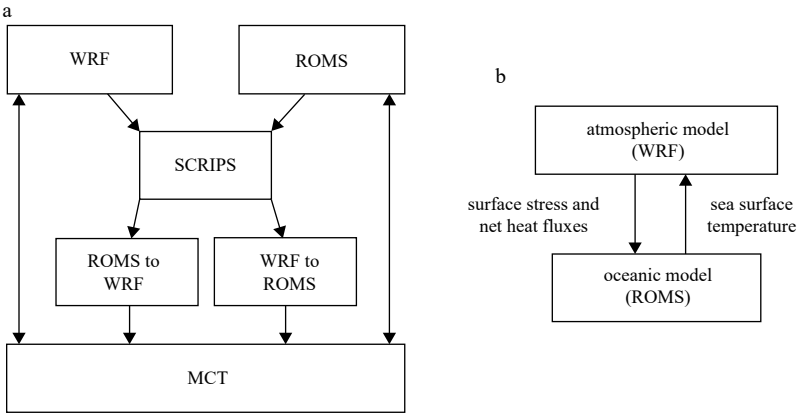

Fig. 1. Schematic of model coupling. a. System flow of the coupled model based on MCT and SCRIPS, and b. configuration of data fields exchanged between WRF and ROMS.

where z_0 is the roughness length, z_c is the Charnock parameter and it is a dimensionless parameter with value of 0.018, u_* is the friction velocity (in m/s), and g is gravity acceleration.

The WRF-ROMS coupling program is developed based on an open-source package named "wrf_roms-1.2.tar.gz", which was downloaded from http://nctr-people.pmel.noaa.gov/-cmoore/wrf-roms/index.html. The developed computational code can be run in either serial or parallel computers, using shared or distributed memory computer architectures. Simulations for two types of storm surges are carried out on distributed memory parallel computers.

3 Model setup

For ROMS ocean model, a third-order upstream horizontal advection scheme is chosen for momentum equations. Mellor-Yamada 2.5 closure is utilized for vertical mixing. Bottom stress is parameterized with a quadratic drag representation and the drag coefficient is set to 0.012. The ocean topography is obtained by combination of two topographic datasets, the 1-min resolution bathymetry data from the National Geophysical Data Center (NGDC) of the NOAA (National Oceanic and Atmospheric Administration) and the 1-min digital bathymetry data from Sung Kyun Kwan University (SKKU) (Choi et al., 2002). The topography is smoothed with three iterations of a second-order Shapiro filter. In addition, NOAA's World Vector Shoreline (WVS) is taken as the coastline.

About the lateral boundary conditions, the open boundary condition and closed boundary condition are employed. On the open boundary, the free surface condition, the two-dimensional (2D) momentum condition and the three-dimensional (3D) momentum radiation condition are given. The time-dependent water elevations and depth-averaged velocities consist of eight main astronomical tides, including M_2, S_2, N_2, K_2, K_1, O_1, P_1 and Q_1. On the close boundary, wall boundary condition is chosen for the sea surface elevation and the normal velocity. The simulations start with a cold start. The initial water level is the mean sea level and the initial flow velocity is zero. In addition, the time-dependent and spatially varying atmospheric wind stresses and net heat fluxes are treated as the surface boundary for ROMS ocean model.

For WRF atmosphere model, the summary of the WRF model configurations used here is given in Table 1. The transferred data between ocean and atmosphere models are exchanged every 10 minutes.

The initial and lateral boundary conditions for WRF model are derived from the ERA-Interim/ECMWF (European Centre for Medium-Range Weather Forecast) reanalysis data with 0.5° spatial resolution and 6 h time resolution. Much research indicates that vortices contained in global reanalysis data are often weak because of the limitation of the resolution (Nguyen and Chen, 2010; Cha and Wang, 2013). In order to forecast the TC track and intensity changes accurately, it always requires accurate representation of the tropical cyclone vortex in the initial WRF conditions. For the purpose of generating better initial typhoon conditions, the TC-Bogus scheme is employed (Hsiao et al., 2010). The original typhoon from the initial atmospheric condition derived from the reanalysis data is removed firstly and then a new typhoon condition based on a Rankin vortex is created (Kurihara et al., 1995).

Table 1. WRF model options

Options	Scheme used in WRF run
Time integration scheme	Runge-Kutta third-order scheme
Spatial differencing scheme	Fifth-order left differencing scheme
Microphysics	Lin scheme
Cumulus parameterization	Kain-Fritsch scheme
Longwave radiation	Rapid Radiative Transfer Model
Shortwave radiation	Dudhia scheme
Land surface	Noah land surface model
Surface layer	Monine-Obukhov scheme
Surface and boundary layers	Yonsei University scheme

$$V = \beta F(r), \tag{2}$$

$$F(r) = \begin{cases} \dfrac{V_m}{r_m} r & (r \leqslant r_m), \\ \dfrac{V_m}{r_m^{\alpha}} r^{\alpha} & (r > r_m), \end{cases} \tag{3}$$

where V is the wind velocity, V_m denotes the maximum wind speed during the typhoon, r_m is the radius from the typhoon center to the point where the maximum wind speed is generated, α is a constant and the value is –0.75, and β is a scale factor.

4 Results and discussion

4.1 *Extratropical storm surge*

A famous extratropical storm surge happened in October

2003 is one of the most severe storm surges in the Bohai Sea caused by the cold-air outbreak (Zhao and Jiang, 2011; Ding and Ding, 2014; Mo et al., 2016). The cold air coming from the Siberia blows through the Bohai Sea. A vast area was struck and the storm surge caused widespread destruction. The storm surge caused by the cold-air outbreak in October 2003 is simulated firstly.

The domain and topography for WRF model are shown in Fig. 2. The domain roughly extends from 29.0°N to 42.5°N in latitude and 112.5°E to 130.5°E in longitude. The model horizontal spacing is 10 km. Sizes of model grid are 150×150. There are 44 uneven σ levels in the planetary boundary layer.

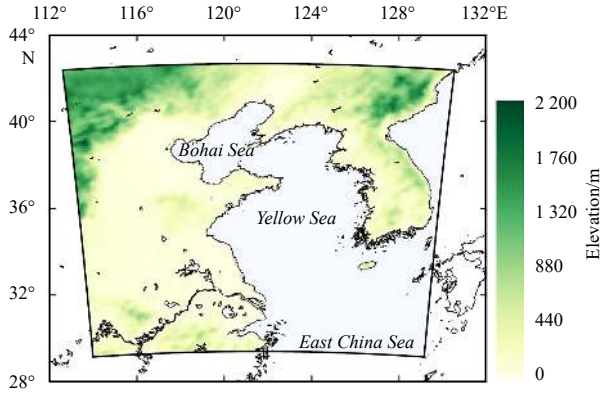

Fig. 2. WRF model domain and the terrain elevation.

Figure 3 shows the domain and bathymetry used in ROMS model. The domains used in two coupled models are large enough to minimize the open boundary effects on study area. The model domain has one open boundary on the southern side and three close boundaries on the other sides. The ROMS domain covers the entire Bohai Sea and the most of the Yellow Sea (35°–41°N, 117°–127°E), which has a spatial resolution of 0.04° and 0.04° in latitude and longitude, respectively. There are totally 250×150 grid points. Six sigma levels are used in the vertical direction.

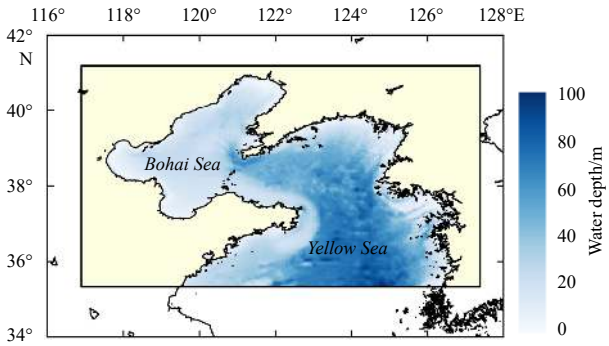

Fig. 3. ROMS model domain and the bathymetry.

The coupled atmosphere model and ocean model are simulated from October 7 to 12, 2003. The Universal Time Coordinated (UTC) is adopted in present paper. In ocean model, the time step for the external (barotropic) mode is 30 s and the time-step ratio of internal (baroclinic) mode to external mode is set to 10. The time step is set to 60 s in atmosphere model. The two models are synchronized 10 min to exchange data fields.

Simulation results are analyzed as follows. Figure 4 shows the wind intensity and direction results from WRF with 12 h's interval, in which the wind over the northern East China Sea is shown. During the starting stage of storm surge (defined as the time before 0900 UTC 10 October 2003), the wind speed over the Bohai Sea was less than 10.0 m/s and there was no obvious rule for the wind direction. And then the wind changed to strong northeasterly during the developed stage (defined as the time between 0900 UTC 10 October and 2100 UTC 11 October) and the wind speed over the northern regions of the Bohai Sea could be larger than 20.0 m/s. During the ending stage (defined as the time after 2100 UTC 11 October 2003), the northeasterly wind over the Bohai Sea became weaker and the wind direction was from northeast to north-northeast.

In order to verify the accuracy of the wind simulation, the time series of computed wind speed at Huanghua Station are compared with observations (Fig. 5). In this figure, the wind speeds derived from the uncoupled model and the ERA-Interim reanalysis data are also shown. The wind speed obtained by the coupled atmosphere-ocean model is in good agreement with the observation data. The simulation results of uncoupled model (WRF only) show a slightly low than those calculated by coupled model in the course of storm surge and the wind speed derived from reanalysis data is much less than the observed data. In addition, based on the wind speed calculated by coupled model, it can be seen that the wind intensity increased quickly before 2000 UTC 10 October. The maximum wind intensity occurred at nearly 2000 UTC 10 October and kept nearly 20 h. The maximum wind speed was over 20 m/s. After 1600 UTC 11 October, the wind speed began to decrease.

In order to assess the simulation results, the Root Mean Square Error (RMSE) and the Normalized Root Mean Square Error (NRMSE) indices are introduced:

$$\mathrm{RMSE} = \sqrt{\frac{\sum_{n=1}^{N} (\widehat{y}_n - y_n)^2}{N}}, \tag{4}$$

$$\mathrm{NRMSE} = \frac{\mathrm{RMSE}}{y_{\max} - y_{\min}}, \tag{5}$$

where N is the number of observation data. $\widehat{y}_n$ is the simulated result and y_n is the measured data. $y_{\max}$ and $y_{\min}$ are defined as the maximum value and the minimum value of the measured data, respectively.

The RMSE and NRMSE as well as biases for wind speed are presented in Table 2. Compared with biases, it indicates that all the methods have a trend to underestimate the wind speed. The coupled atmosphere-ocean model shows good accuracy in reproducing the wind speed with NRMSE lower than 12%. Simulations using the WRF only model are slightly weaker than those calculated by coupled model. The RMSE and NRMSE for uncoupled model are little bigger than those of coupled model. The results indicate that the sea surface temperature is not very important to the numerical simulation of cold-air outbreak. The reanalysis data is negatively biased up to 6.73 m/s. Bruneau and Toumi (2016) also found that the blended sea wind data may significantly under-estimate the extreme winds.

The storm surge's magnitude mainly depends on the wind stress. Figure 6 shows the intensity and direction of 12-h average wind stress in the Bohai Sea and the north of the Yellow Sea. Dur-

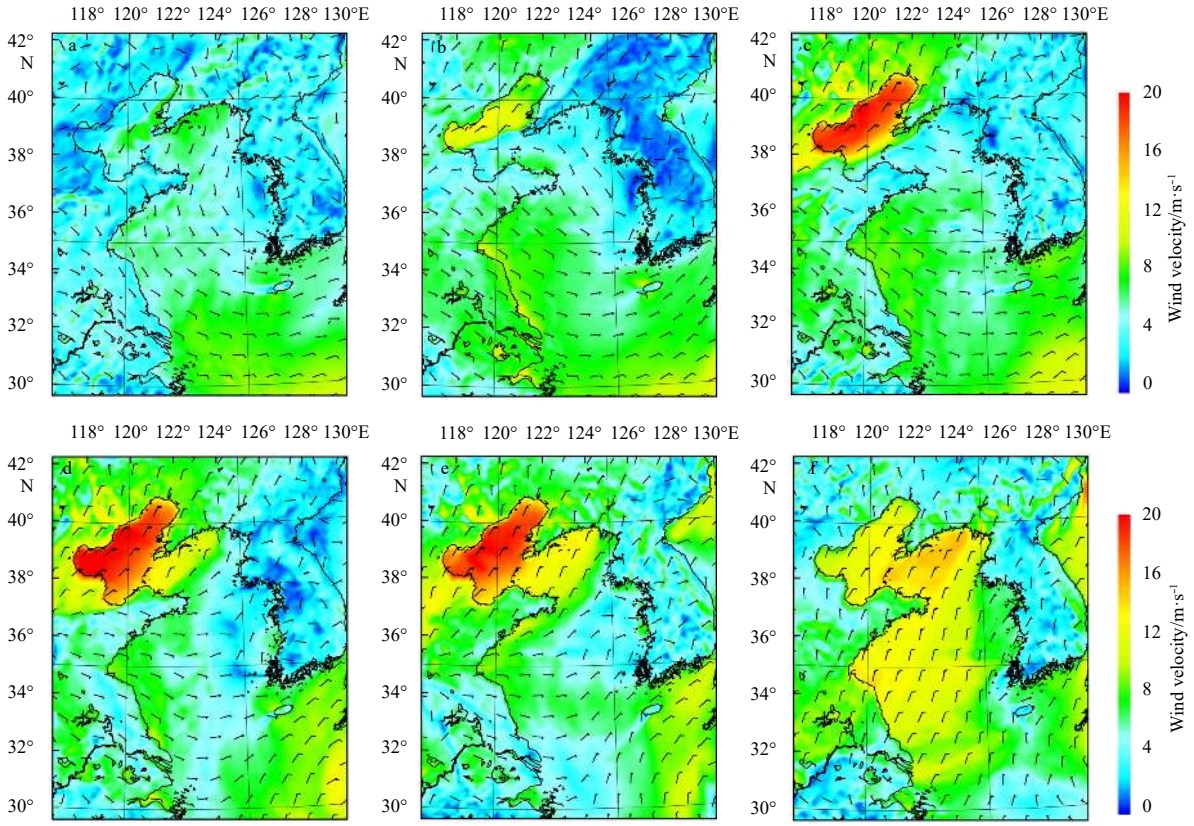

Fig. 4. Wind intensity and direction results from WRF. a. 2100 UTC 9 October 2003, b. 0900 UTC 10 October 2003, c. 2100 UTC 10 October 2003, d. 0900 UTC 11 October 2003, e. 2100 UTC 11 October 2003, and f. 0900 UTC 12 October 2003.

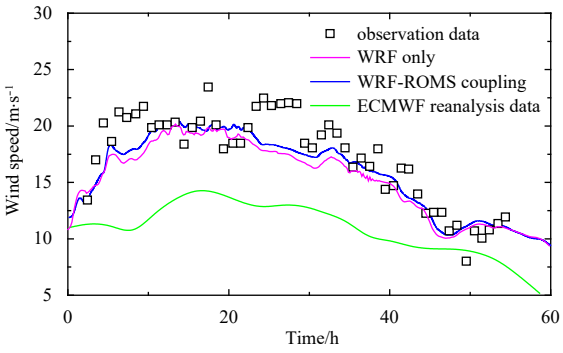

Fig. 5. Comparison of the observed (black squares) and computed (blue line and pink line) wind speed time series. The ECMWF ERA-Interim reanalysis data is included (green line). The time begins at 1000 UTC 10 October 2003

Table 2. Statistical result of the wind speed

Methods	Wind speed	
	RMSE (NRMSE)	Bias/m·s^{-1}
Coupled model	1.76 (11.4%)	–1.00
WRF only	2.04 (13.2%)	–1.40
Reanalysis data	7.14 (46.2%)	–6.73

ing the starting stage of storm surge, the average wind stress over the Bohai Sea was less than 0.1 N/m^2. During the developed stage, the wind stress became much larger and the value of wind stress in mid-west of the Bohai Sea could be larger than 1.2 N/m^2 on October 11, 2003. During the ending stage, the average wind stress began to decrease and the direction is northeast by north.

The mean surface flow velocity is directly affected by the wind stress. The 12-h average surface currents are calculated by ROMS (Fig. 7). During the starting stage of extratropical storm surge, the mean surface velocity in Bohai Bay was lower than 0.2 m/s and the direction of the tidal currents was the unidirectional flow at the Bohai Strait. During the developed stage, the spatial characteristics of the surge surface current became more complicated and the direction of the currents was counterclockwise at the Bohai Strait. The currents flowed into the Bohai Sea from the north of the Bohai Strait and flowed out from the south of the strait. The mean currents in the northeast of the Bohai Sea flowed out of the Liaodong Bay, while the currents in the central area flowed into the Bohai Bay and Laizhou Bay. The maximum mean velocity occurred near the north coast of the Bohai Sea and the velocity was larger than 1.0 m/s. These trends were maintained for nearly 36 h. During the ending stage, the mean velocity in the Bohai Sea decreased observably and the current along the coastline of the Yellow Sea traveled to the southwest. The region with larger mean velocity was located in the western area of the north Yellow Sea.

Figure 8 shows the spatial distribution of total sea level derived from ROMS. The largest height of water level was up to nearly 3 m, which occurred along the western coast of the Bohai Bay. Meanwhile, the Liaodong Bay experienced a negative water level of about 2 m. The distribution trend of the maximum water level was gradually increasing from the east to the west in the Bohai Sea. From the previous analysis, in the Liaodong Bay, current flows out of the bay because of the sustained northeast wind and the seawater accumulates mainly in the coastal zone of the west-

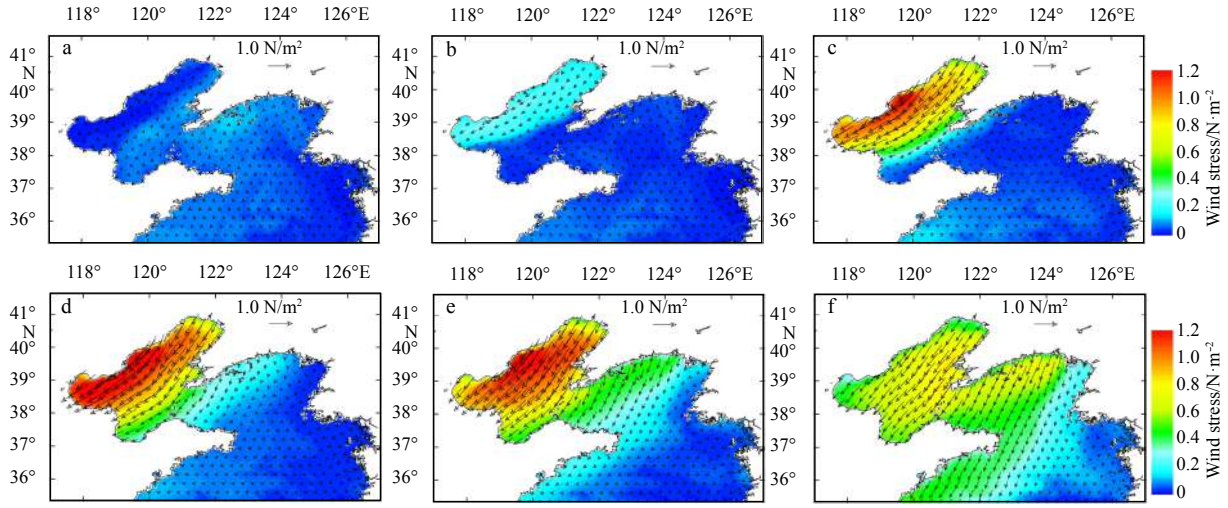

Fig. 6. 12-h average wind stresses from WRF. a. From 1200 UTC to 2400 UTC on 9 October, b. from 0000 UTC to 1200 UTC on 10 October, c. from 1200 UTC to 2400 UTC on 10 October, d. from 0000 UTC to 1200 UTC on 11 October, e. from 1200 UTC to 2400 UTC on 11 October, and f. from 0000 UTC to 1200 UTC on 12 October.

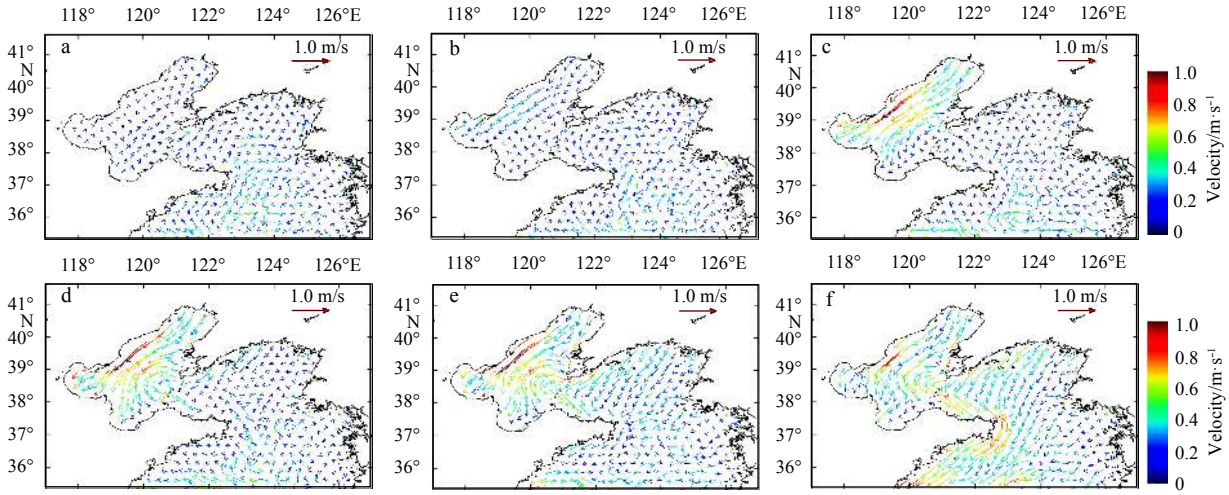

Fig. 7. 12-h average surface currents calculated by ROMS. a. From 1200 UTC to 2400 UTC on 9 October; b. from 0000 UTC to 1200 UTC on 10 October; c. from 1200 UTC to 2400 UTC on 10 October; d. from 0000 UTC to 1200 UTC on 11 October; e. from 1200 UTC to 2400 UTC on 11 October; and f. from 0000 UTC to 1200 UTC on 12 October.

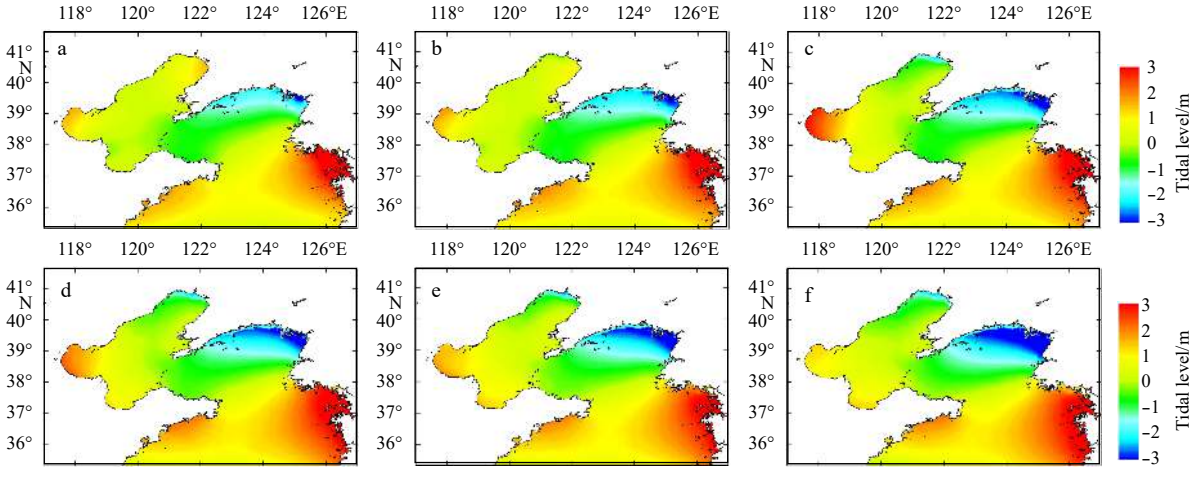

Fig. 8. Spatial distribution of total sea level calculated by ROMS. a. 2100 UTC 9 October 2003, b. 0900 UTC 10 October 2003, c. 2100 UTC 10 October 2003, d. 0900 UTC 11 October 2003, e. 2100 UTC 11 October 2003, and f. 0900 UTC 12 October 2003.

ern Bohai Sea caused by the effect of the geometry. The results indicate that the storm surge's magnitude mainly depends on the intensity and direction wind, but the coastal geometry and bathymetry have a great impact on the magnitude. The northeast direction is the main direction for the extratropical storm surge in the Bohai Sea and the worst affected areas are the Bohai Bay and Liaodong Bay (Kong, 2014; Li et al., 2017).

The comparison between simulations and observations about the water level is shown in Fig. 9. The water level calculated by WRF-ROMS coupling model is consistent with the observations. Tide in west coast of the Bohai Bay area belongs to regular semidiurnal tide. The daily astronomical high tide happened at 9 o'clock and 21 o'clock on October 10. As shown in Fig. 9, the water level peaked at 2100 UTC 10 October 2003 and the largest height of water level was up to 3.12 m. And then the high wave level began to decrease with the tidal oscillations. The interaction between the astronomical tide and the storm surge can be clearly observed. In a word, the combination of wind stress elevation caused by strong northeast wind and the astronomical tide can easily leads to a large extratropical storm surge in the Bohai Sea, which can bring a tremendous security risk to economy and people's lives.

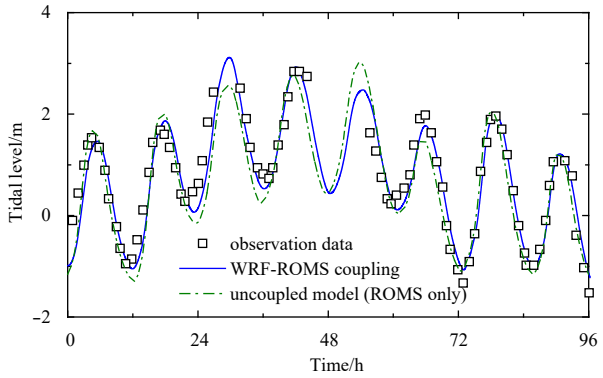

Fig. 9. Observed (black squares) and simulated (blue line and green line) time series of water level at the Huanghua station. The time begins from 1600 UTC 9 October 2003.

Moreover, the simulation results calculated by uncoupled model are also shown in Fig. 9. Li et al. (2016) developed a storm surge numerical model for the Bohai Gulf, where the QSCAT blended wind data was used to calculate the wind stress. It indicates that the error for uncoupled model is evidently greater than that for WRF-ROMS coupling model. The statistics about the water level are presented in Table 3. The coupled model shows globally low RMSE (24 cm, 5.2%) and low unbiased prediction of the water level (6 cm). The NRMSE obtained by the uncoupled model is 9.6% and the model is negatively biased about 18 cm, which indicates that the model trends to obviously underestimate the water level.

4.2 *Typhoon storm surge*

In the summer of 1992, the strong Typhoon 9216 attacked China and caused severe disaster. The typhoon storm surge caused damage on the coast of the East China Sea, Yellow Sea and Bohai Sea. Typhoon 9216, which is also named Typhoon Polly, offers a good case of typhoon that travels a long distance inland and still keeps its intensity. Next, the storm surge caused by Typhoon Polly in 1992 is simulated and analyzed. The results of typhoon storm surge are compared with those of the extratropical storm surge.

Table 3. Statistical result of the water level

Methods	Water level	
	RMSE (NRMSE)	Bias/m
Coupled model	0.24 (5.2%)	−0.06
Uncoupled model	0.44 (9.6%)	−0.18

The track of Typhoon 9216 is shown in Fig. 10. The solid blue line is the best track of the Typhoon Polly and the numbers show time series. The track is from the China Meteorological Administration (CMA) with 6-h tropical cyclone positions. Table 4 shows the observed parameters for the Typhoon 9216. The first time is 0000 UTC 28 August and the last time is 1200 UTC 2 September.

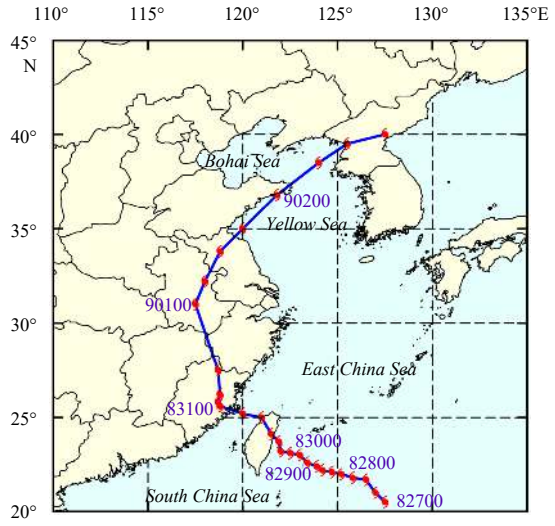

Fig. 10. Track of the Typhoon 9216.

The WRF domain roughly extends from 16.0°N to 47.5°N in latitude and 108.0°E to 142.0°E in longitude (Fig. 11). The WRF model has approximately 15 km horizontal resolution with 44 uneven σ levels in the planetary boundary layer. Sizes of model grid are 185×235. As previously mentioned, the TC-Bogus scheme is used to generate better initial typhoon condition. The settings about the bogus storm are shown in Table 5.

As shown in Fig. 12, the ROMS domain has open boundaries on the southern and eastern sides and closed boundaries are used on the other two sides. The ROMS domain covers the entire Bohai Sea, Yellow Sea and East China Sea and a part of the South China Sea, Japan Sea and Pacific Ocean (20.5°–44.0°N, 115.0°–133.0°E). The ROMS model has approximately 0.05° horizontal resolution with six sigma levels in the vertical direction.

In ROMS ocean model, the time step for the external mode is 30 s and the ratio of internal to external time steps is set to 10. For WRF atmosphere model, the time step is set to 60 s. The two models are initialized at 0000 UTC 29 August 1992 and are synchronized 10 min to exchange data fields.

The wind vectors from the 2100 UTC 30 August to the 0900 UTC 2 September with 12 h's interval are shown in Fig. 13. The results show the propagation of Typhoon Polly through the China's north-eastern coastal areas. The Typhoon 9216 decreased in intensity as it traveled towards the Bohai Sea. With continuous developing of the typhoon, the areas with large wind speed moved northwards and were mainly in the western of the northeast China Sea and northern of the Bohai Sea. The maxim-

Table 4. Observed parameters for the Typhoon 9216

Date	Time (UTC)	Central location/(°)	Central pressure/hPa	Maximum wind speed/m·s^{-1}
Aug. 28, 1992	0000	22.0°N, 125.2°E	985	25
	0600	22.1°N, 124.7°E	985	25
	1200	22.2°N, 124.2°E	985	25
	1800	22.4°N, 123.9°E	980	30
Aug. 29, 1992	0000	22.6°N, 123.4°E	980	35
	0600	23.0°N, 123.0°E	975	35
	1200	23.1°N, 122.5°E	975	35
	1800	23.2°N, 122.0°E	975	35
Aug. 30, 1992	0000	23.7°N, 121.9°E	975	35
	0600	24.1°N, 121.5°E	975	30
	1200	25.0°N, 121.0°E	975	30
	1800	25.2°N, 120.0°E	975	25
Aug. 31, 1992	0000	25.6°N, 118.8°E	978	20
	0600	25.8°N, 118.7°E	982	20
	1200	26.2°N, 118.8°E	986	12
	1800	31.0°N, 117.5°E	988	10
Sep. 01, 1992	0000	32.2°N, 118.0°E	990	10
	0600	33.8°N, 118.8°E	990	12
	1200	35.0°N, 120.0°E	993	12
	1800	36.8°N, 121.8°E	995	12
Sep. 02, 1992	0000	38.5°N, 124.0°E	998	12
	0600	39.5°N, 125.5°E	1 000	10
	1200	40.0°N, 127.5°E	1 000	10

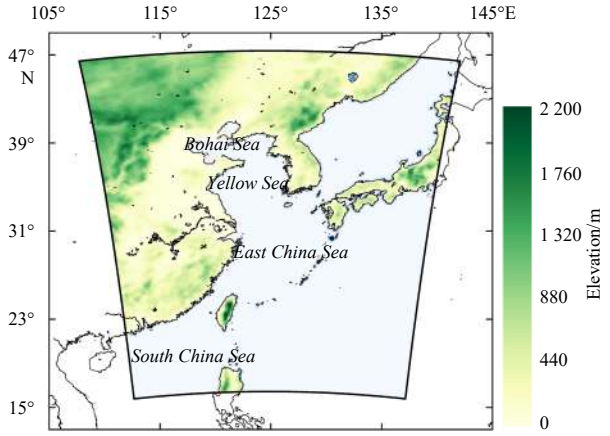

Fig. 11. WRF model domain and the terrain elevation.

Table 5. Bogus settings

Bogus parameter	Value
Latitude of bogus storm/(°)	22.6
Longitude of bogus storm/(°)	123.4
Maximum observed wind speed/m·s^{-1}	35.0
Radius/km	180.0
Scale factor	0.9

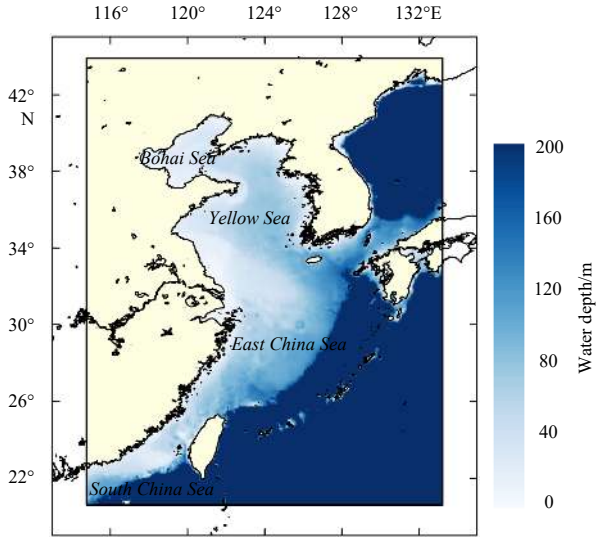

Fig. 12. ROMS model domain and the bathymetry.

um wind speed was faster than 20 m/s. From numerical results, it can be found that the Typhoon 9215, also named Typhoon Omar, was moving westward. Typhoon Omar formed on August 23 from the monsoon trough across the western Pacific Ocean and reached its peak intensity on August 29. Typhoon Omar weakened significantly before striking eastern Taiwan and dissipated gradually.

During cold-air outbreaks (Fig. 4), the strong winds mainly come from the northeast and last for tens of hours. In contrast, the intensity and direction of the typhoon wind are changing significantly in time and the wind field presents as cyclone wind field with large scale.

The time series of minimum sea level pressure (MSLP) calculated by coupled and uncoupled models are compared with the CMA estimations (Fig. 14). The calculation results obtained from WRF-ROMS coupled model show that the MSLP started at approximately 983 hPa on 0000 UTC 29 August and decreased to nearly 973 hPa on 0600 UTC 29 August. After that, the value of MSLP slowly increased with time. The MSLP ended at approximately 1 002 hPa on 1200 UTC 2 September. The comparison shows that the calculated data agree well with the field observa-

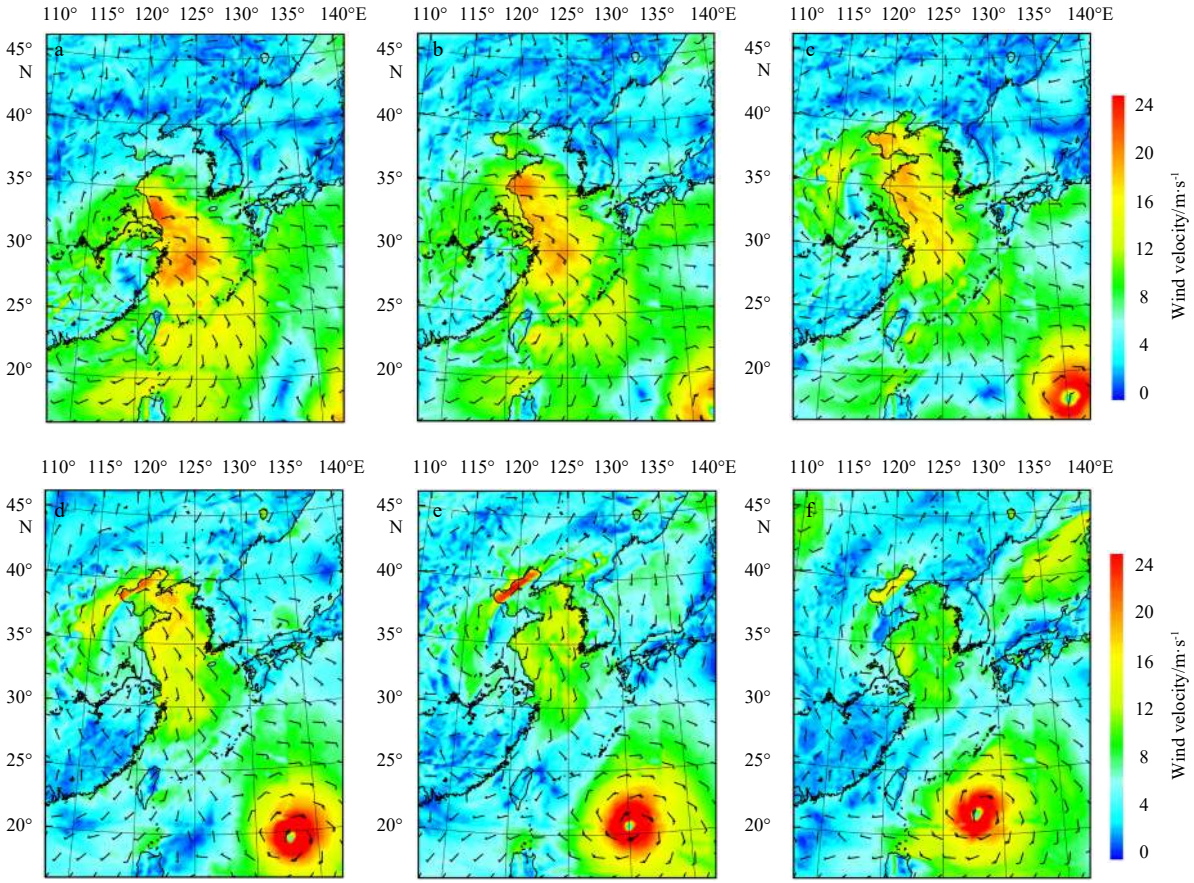

Fig. 13. Wind intensity and direction results from WRF for Typhoon Polly. a. 2100 UTC 30 August 1992, b. 0900 UTC 31 August 1992, c. 2100 UTC 31 August 1992, d. 0900 UTC 1 September 1992, e. 2100 UTC 1 September 1992, and f. 0900 UTC 2 September 1992.

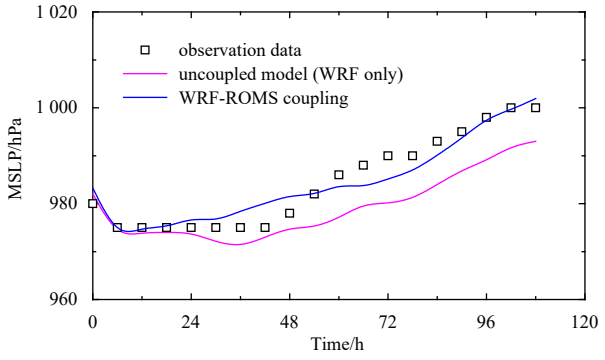

Fig. 14. Time series of observed (black squares) and simulated (blue line and pink line) minimum sea-level pressure. The time begins at 0000 UTC 29 August 1992.

tions. The average absolute error of the MSLP for coupled model is 2 hPa and the NRMSE is 9.1%. It indicates that the ECMWF 0.5 resolution reanalysis data set, TC-Bogus scheme, and WRF physics scheme are suitable for simulating the Typhoon 9216.

The MSLP calculated by uncoupled model (WRF only case) started at approximately 982 hPa on 0000 UTC 29 August and decreased to 971 hPa on 1200 UTC 30 August. Thereafter, the value of MSLP increased with time and the model intensities decreased to nearly 993 hPa on 1200 UTC 2 September. The average absolute error of the MSLP for uncoupled model is nearly 5 hPa and the NRMSE is 25%. This numerical case is actually more intense than observed. The WRF only case is more likely to exaggerate the intensity of the hurricane (Warner et al., 2010). The simulation result indicates that the intensity of typhoon is sensitive to the sea surface temperature and the coupled model can simulate the typhoon more accurately.

The average stress from WRF model demonstrates strongly connection with the location of the Typhoon Polly. The intensity and direction of 12-h average wind stress in the northeast China Sea are shown in Fig. 15. The areas with large wind stress were mainly located in the western of the northeast China Sea. The maximum wind stress in the middle of the East China Sea was larger than 1.2 N/m^2 on 30 August and the stress direction was toward the land. Since then, the wind stress in the Yellow Sea gradually decreased and the wind stress in the Bohai Sea increased with the typhoon traveling northerly. Meanwhile, the direction of the wind stress counter-clockwise deflected.

Owing to the characteristics of the cyclone wind field, the value and direction of the wind stress change quickly with the development of typhoon. The regions with larger wind stress mainly distribute in the north of the Bohai Sea during typhoon storm surge. Different from these characteristics, the wind stress values on most areas of the Bohai Sea are high and the stress direction changes little during extratropical storm sure (Fig. 6).

As the typhoon storm surge developed, the wind-driven surface currents became stronger. The 12-h average surface currents are used to estimate the wind-driven currents in the study area, which are shown in Fig. 16. During the typhoon moving northward, the maximal intensity of average surface current was

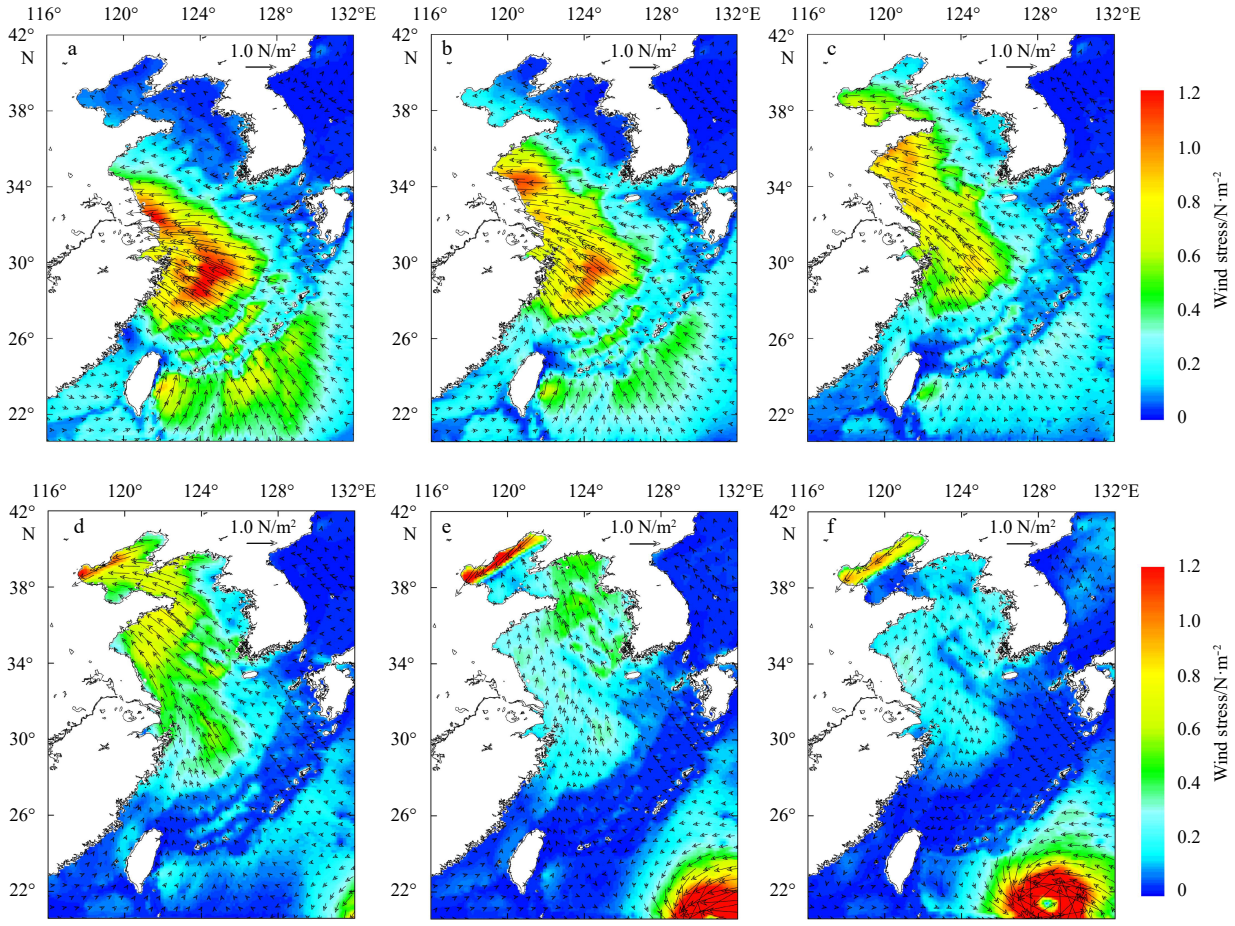

Fig. 15. 12-h average wind stresses from WRF for Typhoon 9216. a. From 1200 UTC to 2400 UTC on 30 August, b. from 0000 UTC to 1200 UTC on 31 August, c. from 1200 UTC to 2400 UTC on 31 August, d. from 0000 UTC to 1200 UTC on 1 September, e. from 1200 UTC to 2400 UTC on 1 September, and f. from 0000 UTC to 1200 UTC on 2 September.

reached on 1 September, with value up to 1 m/s in the north coastal area of the Bohai Sea. In consistent with the wind stress results, the direction of the average surface currents in Yellow Sea also counter-clockwise deflected.

There are distinct differences in the flow structure between extratropical storm surge and typhoon storm surge (Figs 7 and 16). During the typhoon storm surge, the direction of the average surface currents is the unidirectional flow at the Bohai Strait. Furthermore, before the water level reaches to the peak value, the average surface current flows into the Bohai Sea via the Bohai Strait. Subsequently, the average surface current flows out from the Bohai Sea.

The spatial distribution of water level obtained from ROMS for Typhoon Polly is shown in Fig. 17. The largest height of water level in the Bohai Sea was greater than 3 m, which occurred along the western coast of the Bohai Bay and the eastern coast of the Liaodong Bay. The values of maximum water level were lower in middle of the Bohai Sea and higher in east and west of the Bohai Sea. The magnitude of typhoon storm surge mainly depends on the intensity and the track of the typhoon. During the typhoon storm surge, due to the characteristics of the coastal geometry and submarine topography, the seawater accumulated mainly in the coastal zone of the western and eastern Bohai Sea and the worst affected areas were the Bohai Bay and Liaodong Bay. Therefore, the storm surge is mainly determined by the ocean surface driving force, but greatly influenced by the coastal geometry and bathymetry.

The distribution trend of water level for extratropical storm surge has a clear difference with that for typhoon storm surge (Figs 8 and 17). During typhoon storm surge, the Bohai Bay and Liaodong Bay experience the positive storm surge simultaneously. In contrast, the Bohai Bay experiences a positive storm surge, while the Liaodong Bay experiences a negative storm surge during extratropical storm surge.

As shown in Fig. 18, the water level series between simulations and observations are compared. As with the extratropical storm surge, the high tide level decreased with the tidal oscillations after the peak appearance. The results calculated by coupled model are consistent with the observation data. The highest storm surge occurred at the same time as the peak surge coinciding with the daily astronomical high tide. The calculated water level peaked at 0900 UTC 1 September 1992 and the largest height was up to 3.2 m. The absolute error of the largest height between simulations and observations is 0.2 m and the NRMSE for WRF-ROMS coupled model is 6.4%. The model is negatively biased around 10 cm, which indicates that the coupled model trends to underestimate the water level globally. In order to reduce the calculation error, the influence of wave should be considered in the future research (Warner et al., 2010; Feng et al., 2011). In Fig. 18, the results calculated by uncoupled model

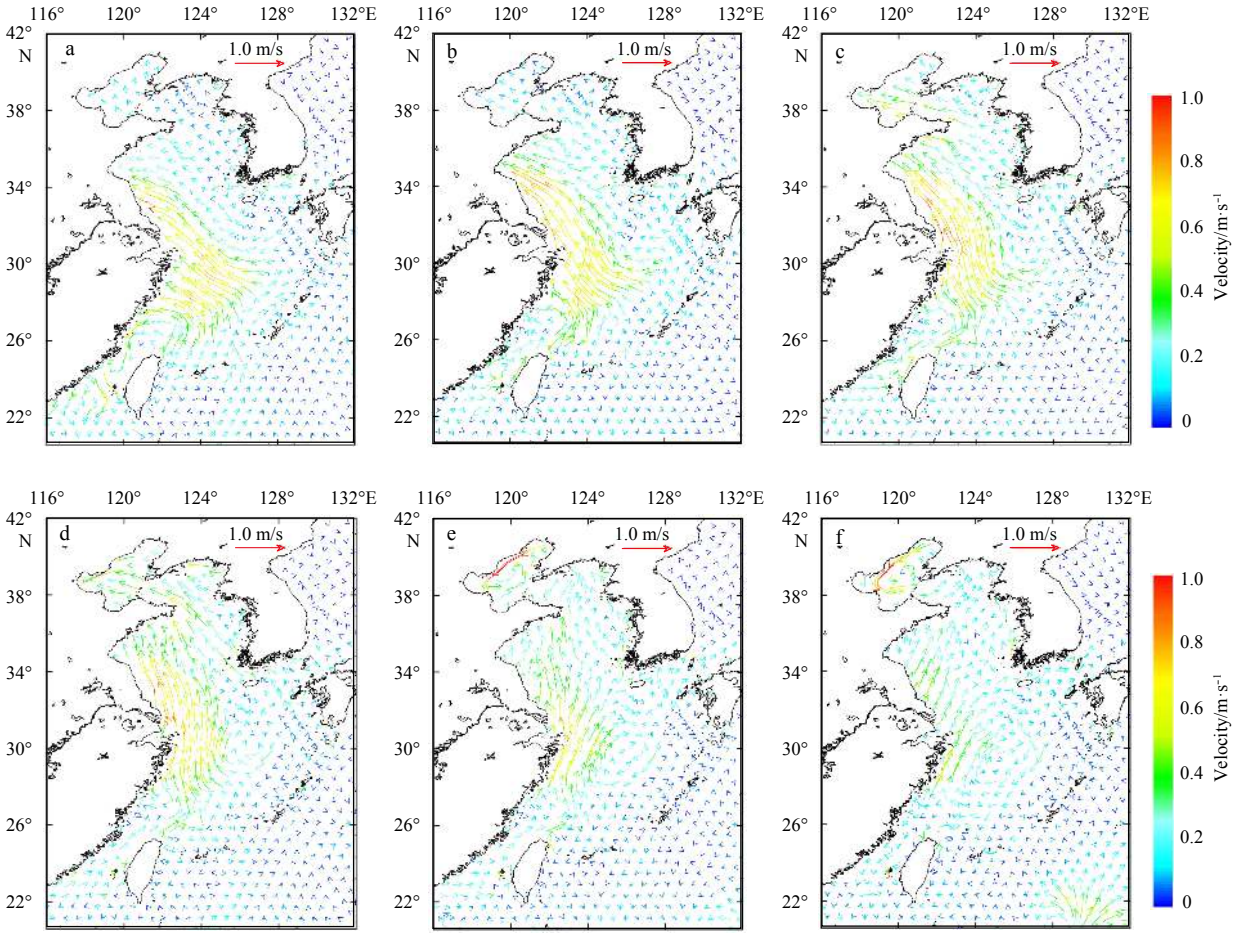

Fig. 16. 12-h average surface currents calculated by ROMS. a. From 1200 UTC to 2400 UTC on 30 August, b. from 0000 UTC to 1200 UTC on 31 August, c. from 1200 UTC to 2400 UTC on 31 August, d. from 0000 UTC to 1200 UTC on 1 September, e. from 1200 UTC to 2400 UTC on 1 September, and f. from 0000 UTC to 1200 UTC on 2 September.

(ROMS only) are also shown and the extreme water level is obviously lower than that obtained by coupled model. The NRMSE for ROMS only model is 10.9%.

Through comparison between Fig. 9 and Fig. 18, it can be seen that the typhoon storm surge comes and goes quickly, while the extratropical storm surge is relatively long-lasting. The reason for the difference is the distinct characteristics of wind field for two types of storms. The strong wind always lasts for tens of hours during cold-air outbreak, while the duration of strong wind over the Bohai Sea during typhoon event is short.

5 Conclusions

A coupled atmosphere-ocean model is developed to study the two types of storm surges induced by extratropical storm and tropical cyclone in the Bohai Sea. The coupled model is comprised of ocean model (ROMS) and atmosphere model (WRF). The open-source software packages of MCT and SCRIP are used to realize data exchange between the two models with independent grids. The wind filed and MSLP obtained from WRF agree well with the observed data. The total sea levels computed by ROMS during storm surges are also in good agreement with the tide gauge observations. The computational domains, model settings, physics schemes and reanalysis data from ECMWF are suitable to simulate the extratropical storm surge occurred in October 2003 and the typhoon storm surge occurred in August 1992. In addition, the TC-Bogus scheme is reasonable for simulating the typhoon storm surge. Generally, the simulation results of atmosphere and ocean gained by coupled model are better than those obtained by uncoupled model.

Storm surges usually occur at the same time as the peak surge coinciding with the astronomical high tide. The magnitude of extratropical storm surge mainly depends on the intensity and direction of the sustained wind, while the magnitude for typhoon storm surge mainly depends on the intensity and the track of the typhoon. The wind field has great differences between extratropical storm surge and typhoon storm surge in the Bohai Sea. Compared with cold-air outbreaks, the intensity and direction of the typhoon wind are changing significantly in time. There are strong links between the average wind stress and the location of the typhoon. There are also obviously differences in the flow structure between extratropical storm surge and typhoon storm surge. The direction of the average surface current is the unidirectional flow at the Bohai Strait during the stage of typhoon storm surge. Meanwhile, the distribution trend of total sea level for typhoon storm surge has quite difference with that for extratropical storm surge. The Bohai Bay and Liaodong Bay experience the positive storm surge simultaneously during typhoon storm surge, but the Liaodong Bay experiences a negative storm surge during extratropical storm surge.

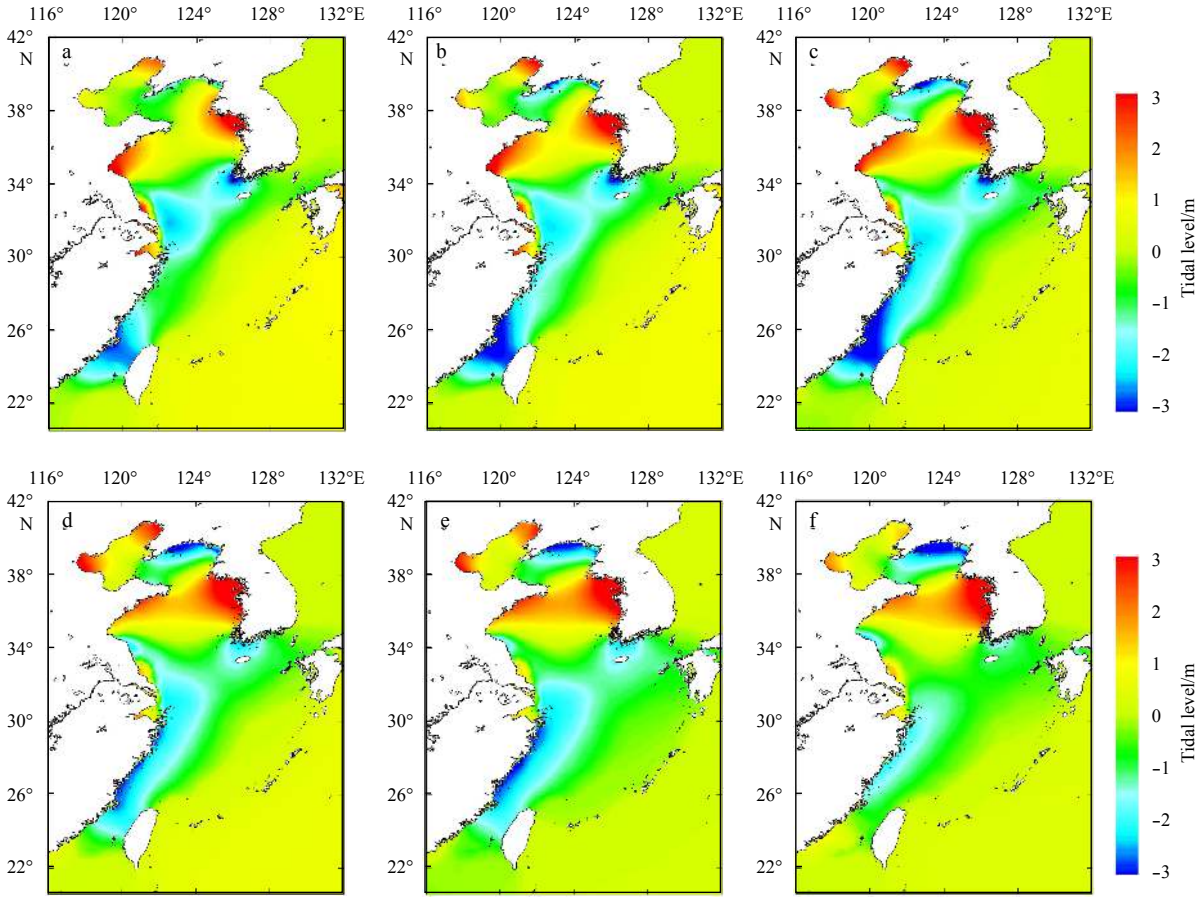

Fig. 17. Spatial distribution of water level from ROMS for Typhoon 9216. a. 2100 UTC 30 August 1992, b. 0900 UTC 31 August 1992, c. 2100 UTC 31 August 1992, d. 0900 UTC 1 September 1992, e. 2100 UTC 1 September 1992, and f. 0900 UTC 2 September 1992.

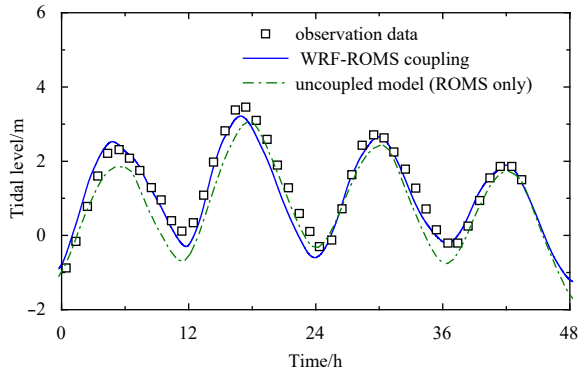

Fig. 18. Comparison of water level between simulations (blue line and green line) and observations (black squares) at Tanggu station. The time begins at 1600 UTC 31 August 1992.

Acknowledgements

We are grateful to NCAR, which is responsible for the WRF model. The authors are also grateful to Rutgers University and University of California at Los Angeles (UCLA), which are responsible for the ROMS model. Furthermore, the open-source package named 'wrf_roms-1.2.tar.gz' provides a favorable technique foundation for developing WRF-ROMS coupling system. The MCT is accessible from http://www.mcs.anl.gov/research/projects/mct and the SCRIP can be obtained from http://oceans11.lanl.gov/trac/SCRIP. The ERA-Interim/ECMWF reanalysis data used in present work is available from https://www.ecmwf.int/en/forecasts/datasets/reanalysis-datasets/era-interim.

References

Bruneau N, Toumi R. 2016. A fully-coupled atmosphere-ocean-wave model of the Caspian Sea. Ocean Modelling, 107: 97–111, doi: 10.1016/j.ocemod.2016.10.006

Cha D H, Wang Yuqing. 2013. A dynamical initialization scheme for real-time forecasts of tropical cyclones using the WRF model. Monthly Weather Review, 141(3): 964–986, doi: 10.1175/MWR-D-12-00077.1

Charnock H. 1955. Wind stress on a water surface. Quarterly Journal of the Royal Meteorological Society, 81(350): 639–640

Choi B H, Kim K O, Eum H M. 2002. Digital bathymetric and topographic data for neighboring seas of Korea. Journal of Korean Society of Coastal and Ocean Engineers, 14(1): 41–50

Ding Yumei, Ding Lei. 2014. A numerical simulation of extratropical storm surge and hydrodynamic response in the Bohai Sea. Discrete Dynamics in Nature and Society, 2014: 282085

Ding Yumei, Wei Hao. 2017. Modeling the impact of land reclamation on storm surges in Bohai Sea, China. Natural Hazards, 85(1): 559–573, doi: 10.1007/s11069-016-2586-4

Feng Xingru, Yin Baoshu, Yang Dezhou, et al. 2011. The effect of wave-induced radiation stress on storm surge during Typhoon Saomai (2006). Acta Oceanologica Sinica, 30(3): 20–26, doi: 10.1007/s13131-011-0115-6

Fu Cifu, Dong Jianxi, Wu Shaohua, et al. 2011. Numerical simulation on typical extratropical storm surge in the Bohai Sea. Marine Forecasts (in Chinese), 28(5): 1–8

Fu Cifu, Yu Fujiang, Wang Peitao, et al. 2013. A study on extratropical

storm surge disaster risk assessment at Binhai New Area. Haiyang Xuebao (in Chinese), 35(1): 55–62

Fu Cifu, Fu Xiang, Wu Shaohua, et al. 2014. Numerical simulation study on deepwater channel influenced by negative storm surge and its features in Bohai Sea. Haiyang Xuebao (in Chinese), 36(3): 30–38

Guan Hao, Zhou Lin, Xue Yanguang, et al. 2012. An applied study on the atmosphere-ocean-wave coupled model in the South China Sea. Journal of Tropical Meteorology (in Chinese), 28(2): 211–218

Haidvogel D B, Arango H, Budgell W P, et al. 2008. Ocean forecasting in terrain-following coordinates: formulation and skill assessment of the regional ocean modeling system. Journal of Computational Physics, 227(7): 3595–3624, doi: 10.1016/j.jcp.2007.06.016

Hsiao L F, Liou C S, Yeh T C, et al. 2010. A vortex relocation scheme for tropical cyclone initialization in advanced research WRF. Monthly Weather Review, 138(8): 3298–3315, doi: 10.1175/2010MWR3275.1

Kong Xiangpeng. 2014. A numerical study on the impact of tidal waves on the storm surge in the north of Liaodong Bay. Acta Oceanologica Sinica, 33(1): 35–41, doi: 10.1007/s13131-014-0430-9

Kurihara Y, Bender M A, Tuleya R E, et al. 1995. Improvements in the GFDL hurricane prediction system. Monthly Weather Review, 123(9): 2791–2801, doi: 10.1175/1520-0493(1995)123<2791:IITGHP>2.0.CO;2

Li Daming, Li Yangyang, Pan Fan. 2015. Coupling model of 2-D variable zone storm surge and waves for Bohai Bay. Journal of Shanghai Jiaotong University (in Chinese), 49(5): 730–736

Li Daming, Xu Yanan, Song Shuangxia, et al. 2010. The study on the effect of wave-radiation stress on storm surge in Bohai Bay. Journal of Hydrodynamics (in Chinese), 5(3): 374–382

Li Yong, Chen Xin, Tian Lizhu, et al. 2017. Numerical simulation of the storm surge in Bohai Bay based on a coupled ocean-atmosphere model. Journal of Shanghai Jiaotong University (in Chinese), 51(12): 1512–1519

Li Yong, Tian Lizhu, Pei Yandong, et al. 2016. Numerical simulation of storm surge inundation in the west zone of Bohai Bay. Geological Bulletin of China (in Chinese), 35(10): 1638–1645

Lim H S, Kim C S, Park K S, et al. 2013. Down-scaled regional ocean modeling system (ROMS) for high-resolution coastal hydrodynamics in Korea. Acta Oceanologica Sinica, 32(9): 50–61, doi: 10.1007/s13131-013-0352-y

Liu Na, Ling Tiejun, Wang Hui, et al. 2015. Numerical simulation of Typhoon Muifa (2011) using a coupled ocean-atmosphere-wave-sediment transport (COAWST) modeling system. Journal of Ocean University of China, 14(2): 199–209, doi: 10.1007/s11802-015-2415-5

Liu Yang, Lin Wenshi, Li Jiangnan, et al. 2017. A numerical simulation of latent heating within Typhoon Molave. Acta Oceanologica Sinica, 36(7): 39–47, doi: 10.1007/s13131-017-1082-3

Mo Dongxue, Hou Yijun, Li Jian, et al. 2016. Study on the storm surges induced by cold waves in the Northern East China Sea. Journal of Marine Systems, 160: 26–39, doi: 10.1016/j.jmarsys.2016.04.002

Nguyen H V, Chen Y L. 2010. WRF simulation of a TC-induced recored-breaking heavy rainfall event over Taiwan. In: Proceedings of the Fifth International Ocean-Atmosphere Conference. Taipei: Chinese-American Oceanic and Atmospheric Association (COAA)

Olabarrieta M, Warner J C, Armstrong B, et al. 2012. Ocean-atmosphere dynamics during Hurricane Ida and NoroIda: an application of the coupled ocean-atmosphere-wave-sediment transport (COAWST) modeling system. Ocean Modelling, 43–44: 112–137, doi: 10.1016/j.ocemod.2011.12.008

Skamarock W C, Klemp J B, Dudhia J, et al. 2008. A description of the advanced research WRF version 3. USA: National Canter for Atmospheric Research

Sun Minghua, Duan Yihong, Zhu Jianrong, et al. 2014. Simulation of Typhoon Muifa using a mesoscale coupled atmosphere-ocean model. Acta Oceanologica Sinica, 33(11): 123–133, doi: 10.1007/s13131-014-0561-z

Sun Wenxin, Feng Shizuo, Qin Zenghao. 1979. Numerical modeling of an ultra-shallow water storm surge (I). Haiyang Xuebao (in Chinese), 1(2): 193–211

Sun Wenxin, Feng Shizuo, Qin Zenghao. 1982. Numerical study on the Bohai Sea wind surges-the zeroth-order dynamical model. Acta Oceanologica Sinica, 1(2): 175–188

Wang Yangjie, Zhang Qinghe, Chen Tongqing, et al. 2016. Application of a coupled atmosphere-ocean-wave model in typhoon process simulation. Journal of Waterway and Harbor (in Chinese), 37(2): 135–141

Warner J C, Armstrong B, He Ruoying, et al. 2010. Development of a coupled ocean-atmosphere-wave-sediment transport (COAWST) modeling system. Ocean Modelling, 35(3): 230–244, doi: 10.1016/j.ocemod.2010.07.010

Warner J C, Perlin N, Skyllingstad E D. 2008. Using the Model Coupling Toolkit to couple earth system models. Environmental Modelling & Software, 23(10–11): 1240–1249, doi: 10.1016/j.envsoft.2008.03.002

Wu Shaohua, Wang Xinian, Dai Mingrui, et al. 2002. The general status of storm surges and the simulation of extratropical storm surges in the Bohai Sea. Haiyang Xuebao (in Chinese), 24(3): 28–34

Zambon J B, He Ruoying, Warner J C. 2014. Investigation of hurricane Ivan using the coupled ocean-atmosphere-wave-sediment transport (COAWST) model. Ocean Dynamics, 64(11): 1535–1554, doi: 10.1007/s10236-014-0777-7

Zhao Peng, Jiang Wensheng. 2011. A numerical study of storm surges caused by cold-air outbreaks in the Bohai Sea. Natural Hazards, 59(1): 1–15, doi: 10.1007/s11069-010-9690-7